[001]- and piezoelectric-[111]-oriented InAs/GaSb structures under hydrostatic pressure

D. M. Symons, M. Lakrimi, R. J. Warburton, R. J. Nicholas, N. J. Mason, and P. J. Walker
Physics Department, Clarendon Laboratory, The University of Oxford, Parks Road, Oxford OX1 3PU, United Kingdom

M. I. Eremets
High Pressure Physics Institute, Russian Academy of Sciences, Troitsk, Moscow Region, 142092 Russia

G. Hill
Department of Electronic and Electrical Engineering, The University of Sheffield, P.O. Box 600, Mappin Street, Sheffield S1 4DU, United Kingdom
(Received 10 January 1994; revised manuscript received 11 March 1994)

Magnetotransport measurements have been carried out under hydrostatic pressure on [001]- and [111]-oriented InAs/GaSb structures grown by metal-organic vapor-phase epitaxy. The system is semimetallic at zero pressure, but as the pressure is increased, electrons, located in the InAs layers, transfer back into the valence band of GaSb and a semimetal-to-semiconductor transition is observed. In double heterojunctions the zero band overlap condition occurs at 14 and 17 kbar for the [001] and [111]A orientations, respectively. The band crossing at the interface has been calculated self-consistently for the two orientations, taking into account the intrinsic and extrinsic origins of the carriers. This band overlap is found not only to be strongly orientation dependent, approximately 60 meV larger in [111]A compared with [001], but also to decrease at rates of 10 and 12 meV/kbar for the [001] and [111]A orientations, respectively. These rates are much larger than those determined from molecular beam epitaxy samples, but closer to the variation with pressure of the band gaps of the bulk materials.

I. INTRODUCTION

InAs/GaSb heterostructures have a type-II band lineup with the bottom of the InAs conduction band lying below the top of the valence band of GaSb. For relatively wide layer thicknesses the confinement energies of the electrons and holes are not large and the system is said to be semimetallic.[1] Charge transfer occurs between the layers, giving a two-dimensional electron gas in the InAs layers and a two-dimensional hole gas in the GaSb layers. The structures grown to date are not in practice totally intrinsic and the electron concentration is usually larger than that of the holes. This difference is attributed to pinning of the Fermi energy level in GaSb by both surface states and impurities,[2] as well as to the presence of donor interface defects.[3] The ratio of electron density to hole density has been found to be much larger, to date, in most samples grown by molecular beam epitaxy (MBE) compared with metal-organic vapor-phase epitaxy (MOVPE). A semimetal to semiconducting transition can be induced by thickness variation of the InAs layers, the application of hydrostatic pressure[4] or high magnetic fields,[5,6] due to the resulting shift of the band edges.

There has recently been a lot of interest in strained layer structures which allow enhanced potential for band engineering due to large changes which occur in the valence band and also due to the formation of a piezoelectric field in [111]-oriented structures.[7] Structures grown with a [111] orientation are known to have modified electrical and optical properties compared with those grown along [001]. For example, in this system where the lattice mismatch is about 0.6%, the carrier densities n_e and n_h are higher in [111] compared with [001] samples and semimetallic behavior is observed at lower InAs thicknesses for the [111] orientation.[8]

In this paper, we report on magnetotransport measurements carried out under hydrostatic pressure on both single wells and superlattices of InAs/GaSb for both the [001] and [111]A orientations. We describe a self-consistent model used to calculate the band overlap from the measured carrier densities in double heterojunction (DHET) structures, which takes into account the intrinsic and extrinsic origins of the carriers. This leads to the important conclusion that the band overlap is orientation dependent. The pressure dependence of the band overlap has been measured using the same technique for the two orientations. Finally, data from superlattice (SL) samples are presented that provide further evidence for the orientation dependence of the band overlap.

II. EXPERIMENTAL RESULTS

The samples were grown on semi-insulating [001]- and [111]A-oriented GaAs substrates using atmospheric pressure MOVPE and were not intentionally doped. The

detailed growth conditions have been optimized to give layers with good electrical quality and morphology of the surfaces. The gas switching at the interface between the InAs and GaSb layers was instantaneous, which is thought to favor the formation of an InSb monolayer interface,[9,10] whose presence has been detected by Raman scattering.[11] The growth of the active layers is always preceded by a GaSb buffer layer of at least 2 μm because of the large lattice mismatch of 6% between GaSb and GaAs. The sample characteristics are given in Table I.

We concentrate first on two GaSb/InAs DHET's with thick GaSb capping layers of 1200 Å so that the InAs well is in the flat band regime. The samples were grown in nominally identical runs on [001]- and [111]A-oriented GaAs wafers. The thicknesses of the InAs wells have been measured by transmission electron microscopy to be 300 Å for [001] and 475 Å for [111]A. The samples have been lithographically processed into Hall bars and studied up to 15 T at 4.2 K in a superconducting magnet. The hydrostatic pressure measurements were made using a clamp pressure cell with a liquid medium. The pressure was applied at room temperature, before cooling slowly to 77 K, and then to 4.2 K by immersing the cell in liquid helium. The pressure was measured *in situ* using a manganin pressure gauge.

Typical experimental recordings of ρ_{xx} and ρ_{xy} are shown in Fig. 1 at zero pressure. The traces show several distinct features. First there is a rapid curvature of the Hall resistivity as a function of magnetic field and second only relatively weak oscillatory features are observed in ρ_{xx}. Both of these are attributed to the presence of two separate charge systems, namely, electrons and holes, where the electrons have a much higher mobility. The Hall resistance traces have been fitted to the classical two carrier expressions,[12] yielding values for the electron and hole densities together with their respective mobilities. A typical fit is shown by the dashed line in Fig. 1 and ignores the quantum oscillations which occur at higher fields. Detailed analysis of the Shubnikov-de-Haas oscillations in the ρ_{xx} traces was also performed by taking a numerical derivative of the resistivity and then Fourier transforming the low field oscillations, as shown in Fig. 2. The periodicities have been used to confirm the

TABLE I. The layer thicknesses and carrier densities of the double heterojunctions (DHET's) and superlattices (SL's) described in the text. The superlattices all have 20 layers, although only 18 are active for the [001] SL, and the carrier densities given are the densities per layer.

Sample	Thicknesses InAs (Å)	GaSb (Å)	Electron density (10^{11} cm^{-2})	Hole density (10^{11} cm^{-2})
[001] DHET	300		7.5	4.0
[111] DHET	475		11.5	5.4
[001] SL	200	200	7.03	3.14
[111] SL *a*	200	200	14.45	6.84
[111] SL *b*	480	960	16.56	3.57

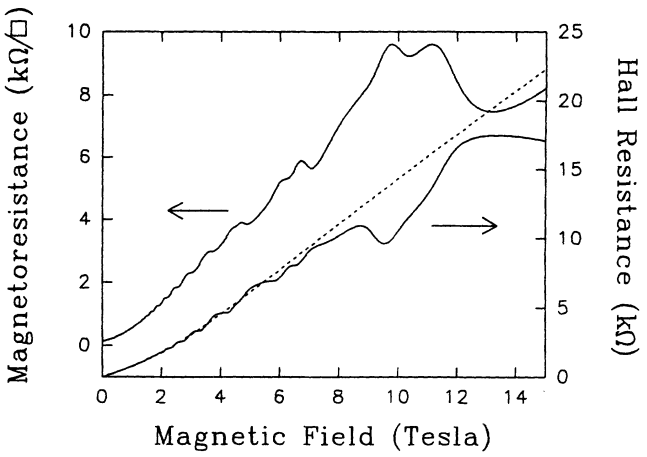

FIG. 1. Hall resistance and magnetoresistance traces for the [001] DHET measured at ambient pressure and 4.2 K. The traces are characteristic of two carrier conduction and the dashed line shows the classical two carrier fit to the measured Hall trace.

fitted values of n_e and also to show that only one subband is occupied. For the [001] ([111]A) DHET the zero pressure electron and hole densities are 7.5 (11.5)$\times 10^{11}$ cm^{-2} and 4.0 (5.4)$\times 10^{11}$ cm^{-2}, demonstrating an enhancement of both n_e and n_h for the [111] sample.

Applying a large hydrostatic pressure causes the band gaps of both materials to increase, causing the band edge energies of the electrons in the InAs and the holes in the GaSb to become closer, thus reducing the band overlap of the two bands. The electrons in the InAs conduction band well transfer back into the GaSb valence band,

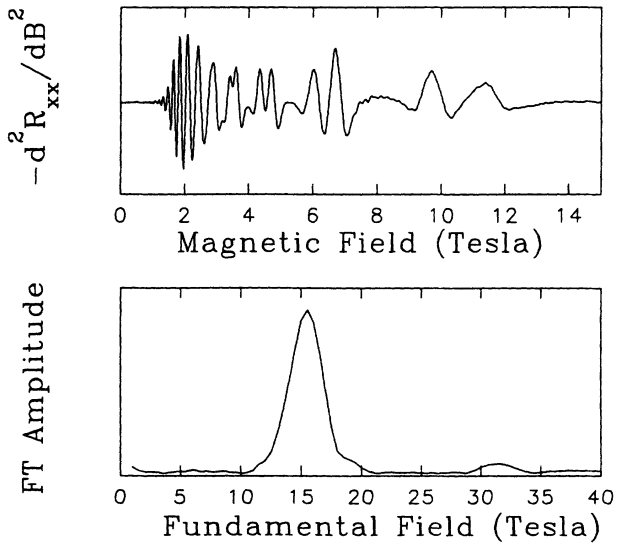

FIG. 2. A typical doubly differentiated zero pressure magnetoresistance trace (top) and the resulting Fourier transform (bottom) which shows very clearly that only one electron subband is occupied.

which results in dramatic changes in the magnetotransport traces as a function of pressure, as shown in Fig. 3. For small pressures, when n_h is still comparable with n_e, the Hall traces still curve up at low magnetic field and have a complicated structure, indicating that both electrons and holes are still contributing to the conduction.[13] As the pressure is further increased, more electrons transfer back to the GaSb valence band, the hole density eventually falls to zero, the low field Hall traces become linear, and quantum Hall plateaus are seen. By approximately 9 kbar all the holes in the sample have disappeared and the conduction is only due to one type of carrier, i.e., the extrinsic electrons. At the same time, the ρ_{xx} traces are seen to change from those which seem to be characteristic for a two carrier system, with only weak oscillatory features and a large low field background magnetoresistance, to the familiar traces characteristic of a single carrier type, with ρ_{xx} falling to zero, or nearly zero, whenever ρ_{xy} exhibits a plateau. A similar change in shape of the traces with pressure was observed by Beerens *et al.*[4] for MBE grown samples.

The variation with pressure of the carrier densities and

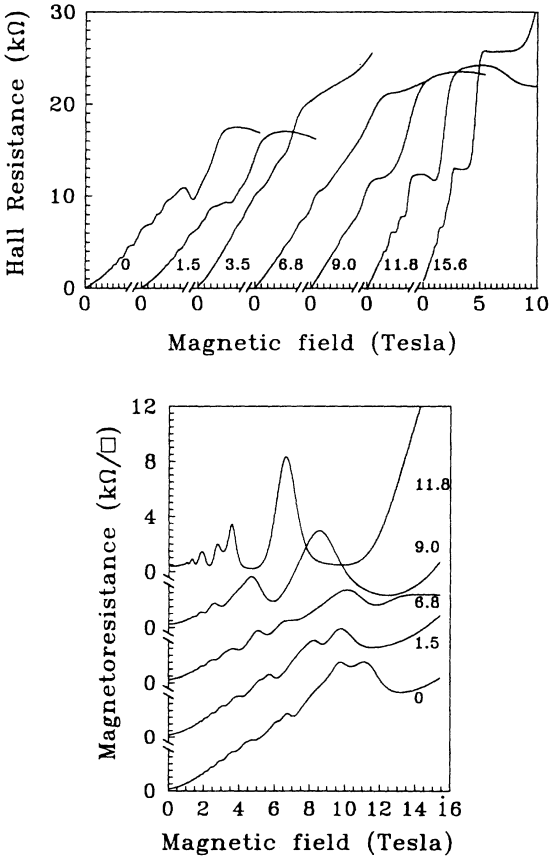

FIG. 3. Hall resistance traces (top) and magnetoresistance traces (bottom) for a [001]-oriented DHET with a 300 Å InAs well. The numbers give the pressure in kbar. As the pressure is increased, a semimetallic to semiconducting transition is observed and the traces are seen to change from those indicating conduction by two carrier types to those characteristic of only one carrier type.

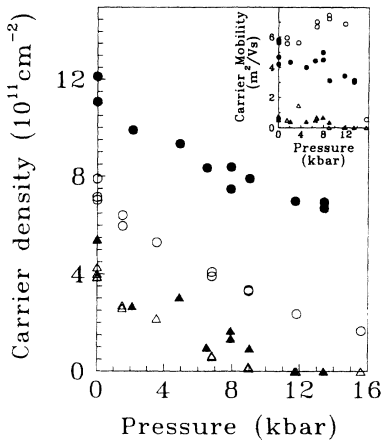

FIG. 4. The densities of electrons (○) and holes (△) for the 300 Å [001] DHET and electrons (•) and holes (▲) for the 475 Å [111]*A* DHET as functions of pressure. The inset shows the electron and hole mobilities as functions of pressure for the same two samples.

mobilities was deduced from similar two carrier fits to those shown in Fig. 1 for the series of pressures studied. This dependence is shown for the DHET samples in Fig. 4. Both the electron and hole densities are seen to decrease with pressure at an approximately constant rate until the hole density reaches zero, which corresponds to the hole confinement energy crossing the Fermi energy. This transition occurs at about 9 kbar for the [001] orientation and 12 kbar for the [111]*A* orientation. As the carrier densities are reduced, the electron mobility, shown in the inset to Fig. 4, is found to increase, probably due to a reduction in the electron-hole scattering. The electron density decreases more slowly, once all the intrinsic carriers have been removed, since the increasing pressure is now only causing the transfer of the extrinsic electrons back into the impurity states or interface defects which produced them. In the following section, we describe a self-consistent calculation of the energy levels and band bending, which is used to estimate the band overlap for both the [001] and [111]*A* orientations, from the fitted carrier densities for the whole pressure range.

III. CALCULATING THE BAND OVERLAPS

A. [001]

From our previous studies we have found that for wide [001]-oriented wells, Fourier transforms of the oscillations in the magnetoresistance show that two electron subbands are occupied with equal, or nearly equal, densities.[14] From this we conclude that the top and bottom interfaces for [001] growth are identical. We have therefore modeled the [001] DHET as a square well modified by the considerable bowing of the bottom of the well, produced by the large density of confined electrons. Since the interfaces are identical it is assumed that half the holes are confined at each interface and that the electric field is zero at the center of the InAs well. The band

overlap is given by the sum of E_0^e (confinement energy of electrons), E_F^e (Fermi energy of electrons), E_0^h (confinement energy of holes), and E_F^h (Fermi energy of holes) as illustrated in Fig. 5.

The electron confinement energy is found using a self-consistent calculation for the electrons confined in the InAs well, taking into account both the energy and pressure dependence of the electron effective mass. This is done by numerically solving Schrödinger's and Poisson's equations as given by

$$\left[-\frac{\hbar^2}{2m_e^*}\frac{d^2}{dz^2}+V(z)\right]\psi_e(z)=E_0^e\psi_e(z)$$

$$\text{for } |z|<\frac{L}{2} \quad , \quad \psi_e(z)=0 \quad \text{elsewhere}$$

$$\frac{d^2\phi(z)}{dz^2}=\frac{en_e}{\epsilon_r\epsilon_0}|\psi_e(z)|^2 \qquad \text{for } |z|<\frac{L}{2} \quad ,$$

where the potential $V(z)=-e\phi(z)$, L is the thickness of the well and n_e is the electron concentration.

We have assumed that the electrons and holes are completely confined in the InAs and GaSb layers, respectively. This is a reasonable assumption in these relatively wide layers because the carriers have to overcome high energy barriers in order to penetrate the adjacent layers and also from considerations of the symmetry mismatch of the band edge wave functions of both kinds of carriers.

A two-band formula for the energy dependence of the electron effective mass in a nonparabolic system is

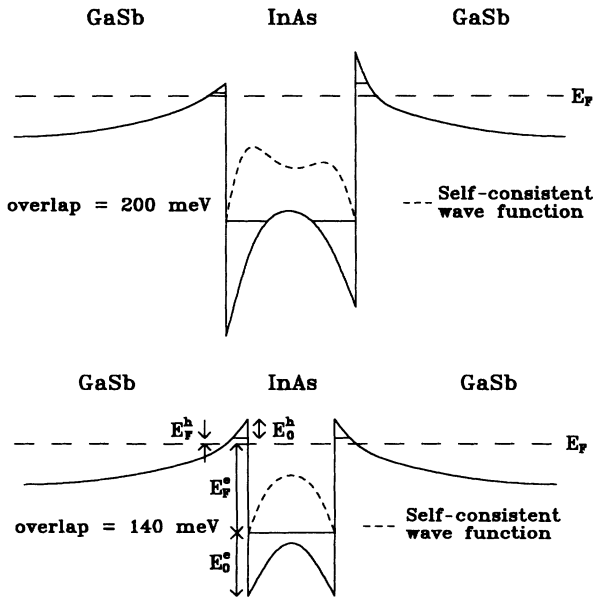

FIG. 5. Band diagram and electron wave function calculated self-consistently for the 300 Å [001] DHET (bottom) and the 475 Å [111]A DHET (top). Only the valence band of GaSb and the conduction band of InAs are shown.

$$m_e^*=m_0^*\left(1-\frac{2K_2E}{E_g}\right),$$

where E is the mean energy relative to the conduction band edge and the nonparabolicity parameter $K_2=-0.86$ for InAs. The band gap E_g and the band edge effective mass m_0^*, as functions of pressure P in kbar, for InAs are

$$E_g=(0.42+0.01P)\,\text{eV},$$

$$m_0^*=\left(0.023+6.67\times10^{-4}P\right)m_0.$$

The Fermi energy of the electrons is given by the familiar expression

$$E_F^e=\frac{\hbar^2\pi n_e}{m_e^*}$$

and different electron effective masses result for motion parallel and perpendicular to the interface, since the degree of nonparabolicity is different in each case.

The hole confinement energy is calculated following the variational method of Ref. 15. The Fang-Howard wave function for holes confined in an inversion layer is

$$\psi_h(z)=\left[\frac{b^3}{2}\right]^{\frac{1}{2}}\left(|z|-\frac{L}{2}\right)e^{-\frac{b}{2}\left(|z|-\frac{L}{2}\right)} \quad \text{for} \quad |z|>\frac{L}{2},$$

which gives the energy of the lowest hole subband as

$$E_0^h=\langle T\rangle+\langle V_s\rangle,$$

where the image potential and the interactions between the holes and the depletion layer charges have been neglected since they are small. The expressions

$$\langle T\rangle=\frac{\hbar^2b^2}{8m_h^{\parallel}},\quad \langle V_s\rangle=\frac{33e^2n_h}{16\epsilon_r\epsilon_0 b}$$

give the expectation values of the hole kinetic energy and the potential energy of a hole interacting with the other holes in the inversion layer, respectively. The variational parameter b is given by

$$b=\left[\frac{33m_h^{\parallel}e^2n_h}{8\epsilon_r\epsilon_0\hbar^2}\right]^{\frac{1}{3}},$$

where n_h is the hole density at each interface, i.e., half the total hole density for this symmetrical [001] case. The effective mass of the holes for motion parallel to the growth direction $m_h^{\parallel}$, which is used in the calculation of the confinement energy, is taken to be $0.3m_0$ for [001] growth and $0.6m_0$ for [111] growth. The effective mass for motion perpendicular to the growth direction $m_h^{\perp}$ is taken to be $0.1m_0$ for both orientations, as measured in similar structures by Sundaram *et al.*,[16] and is used in the expression for the Fermi energy. Energy and pressure dependence of the hole mass are small and have been neglected.

The band overlap at the interface has been calculated for the [001] sample at each pressure and the resulting values are plotted in Fig. 6. At zero pressure the band

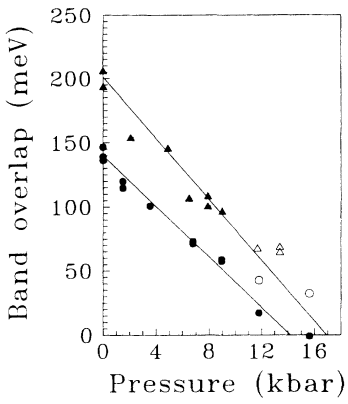

FIG. 6. The calculated band overlaps for the two DHET's as functions of pressure. Filled circles (•) show the [001] overlap with the depletion field in the GaSb taken into account and the open circles (○) show calculated points where this field has been neglected. Filled triangles (▲) show the calculated [111]*A* band overlap but the open triangles (△) only give calculated upper limits, as explained in the text.

overlap is calculated to be 140 meV, which is in good agreement with previously reported values of 150 meV. The low pressure points lie close to a straight line but at higher pressures, once the hole density is zero, the calculation appears to overestimate the band overlap. This is due to the neglect of the depletion field in the *p*-type GaSb. The electron density in the sample is always larger than the hole density but overall the structure is electrically neutral. In the calculation above, it was assumed that the extra positive charge needed to balance the excess of electrons over holes in the structure comes entirely from the two interfaces. In practice, a significant density of positively charged impurities occurs in the depletion regions either side of the InAs well, and this charge must be included in the calculation. In previous calculations it has always been assumed that the interface charge accounts for all the extra positive charge that is needed to satisfy the condition of zero net charge.

The potential energy in the depletion layer is given by the expression[15]

$$V_d(z) = \frac{e^2 N_{\text{depl}}}{\epsilon_r \epsilon_0}\left(|z| - \frac{L}{2}\right)\left(1 - \frac{|z| - L/2}{2z_d}\right),$$

$$\frac{L}{2} < |z| < \frac{L}{2} + z_d$$

where

$$z_d = \left[\frac{2\epsilon_r \epsilon_0 \phi_d}{e(N_A - N_D)}\right]^{\frac{1}{2}}, \quad N_{\text{depl}} = (N_A - N_D) z_d.$$

$N_A - N_D$ is taken to be 1×10^{16} cm^{-3} and ϕ_d is the band bending associated with the depletion layer. While there are holes present ϕ_d is taken to be 34 mV, the potential at which the Fermi energy is found to be pinned in bulk *p*-type GaSb,[17] giving a depletion layer with a charge density of 0.77×10^{11} cm^{-2} on each side of the InAs well. The resulting band diagram at zero pressure is shown in Fig. 5.

In order to predict the behavior beyond the semimetal to semiconductor transition we need to know the interface charge. Since there is no net charge in the structure, the interface charge can be calculated as a function of pressure from the fits in the semimetallic regime. The interface charge is found to remain almost constant with pressure, decreasing by only about 10% between 0 and 10 kbar. By assuming that the interface charge continues to decrease at the same rate beyond the semimetallic to semiconducting transition, we can predict the depletion charge and hence the associated band bending for the two highest pressure values. At these high pressures, when the sample is in the semiconducting regime, the GaSb valence band at the interface lies below the Fermi energy. When the depletion field is included in the calculation of the [001] overlap, all the points are found to lie close to a straight line as shown in Fig. 6. This shows that the band edges of the conduction and valence bands cross at (14±1.5) kbar, leading to the zero overlap condition.

We therefore conclude that the band overlap decreases linearly with pressure at a rate of (9.9±1.0) meV/kbar for the [001] orientation. This rate is significantly larger than previous measurements have deduced. Beerens *et al.*[18] obtained a value of −6.7 meV/kbar using magnetotransport measurements and Claessen *et al.*[19] found this rate to be −5.8 meV/kbar using interband magneto-optical absorption. Both groups used MBE grown samples where n_h is small with respect to n_e. The sample used by Beerens and co-workers had a thin capping layer and a density ratio, n_e to n_h of about 4. When almost all of the carriers are extrinsic the depletion field in the GaSb layers becomes very important. Neglecting this depletion field will lead to a substantial underestimate of this parameter as can be seen from the higher pressure data in Fig. 6, where there is a large discrepancy between the overlaps calculated by the two methods. Our value of (-9.9 ± 1.0) meV/kbar is much closer to the direct band gap pressure coefficients of 10 and 14 meV/kbar for InAs and GaSb, respectively, as would be expected for the pressure coefficient describing the separation of *s* and *p* character bands. More specifically the model-solid theory of Van de Walle and Martin[20] predicts the differential pressure coefficients of the valence bands to be 0.4 meV/kbar, which leads to the prediction that the band crossing should decrease with pressure at (10±3) meV/kbar, which is in good agreement with our experimental results.

B. [111]*A*

In the [111]*A* DHET the diagonal components of the strain tensor are no longer zero, which leads to a calculated piezoelectric field of 3.7×10^4 V cm^{-1} in the InAs well.[21] The structure is no longer symmetric and the proportion of holes on either side of the InAs well must also be calculated. We have assumed, as before, that the extra positive charge needed to satisfy the condition of zero

net charge is made up of both interface charge, which is distributed evenly between the two interfaces, and ionized impurities in the depletion layers. The calculation is similar to the [001] case except that the well is asymmetric. The proportion of holes either side of the well is chosen so that the difference in potential energy of the InAs conduction band at the two interfaces equals the difference in potential energy of the GaSb valence band at the two interfaces. This is equivalent to the requirement that the overlap is equal at the two interfaces. The electric displacement D in the GaSb at a particular interface is determined by the density of holes and the depletion field in the GaSb layer being considered. The depletion field band bending must always be 34 mV if holes are confined at the interface. The value of D at the interface in the InAs layer is then calculated by adding the D field due to the interface charge and the piezoelectric field to the value calculated for the GaSb at the interface. The applied pressure should produce no additional piezoelectric field since, if it is truly hydrostatic, it possesses no defining axis. Also the bulk moduli of GaSb and InAs are almost identical (578 kbar and 580 kbar, respectively) so no additional lattice mismatch is produced by the application of pressure. Therefore the expected piezoelectric field in the InAs layer, neglecting charge transfer, should remain approximately constant with pressure.

At zero pressure it is found that almost all the holes are located at one interface and that the electrons are shifted towards the opposite interface as sketched in Fig. 5. The band crossing at the interface at zero pressure is found to be approximately 200 meV for the [111]A sample, 60 meV larger than for the [001] sample. A similar value for the overlap has been found in a range of different [111]A grown samples, including those with very wide InAs wells when the strain will be relieved and hence there will be no piezoelectric field.[22] If the band overlap were the same for both the [001] and [111]A orientations then in these very wide well samples the carrier density would be independent of crystal orientation. However, the carrier density is found to be consistently about 50% larger for the [111]A than for the [001] samples, which provides further evidence that the band crossing at the interface is in fact larger for the [111]A orientation. Furthermore the semimetallic to semiconducting transition occurs at a higher pressure for [111]A samples, giving additional corroboration that the overlap is larger for the [111]A interface.

Fourier transforms of the ρ_{xx} traces of these very wide well [111]A, strain relieved samples suggest that the two interfaces are identical. This supports, but does not completely justify, our assumption that the interface charge is divided evenly between the interfaces, since the interfaces lie at different energies relative to the Fermi energy. Positively charged impurities must lie above the Fermi energy, so if the interface charge is divided unevenly between the interfaces there must be more charge at the interface which lies at a higher potential. This unequal distribution of interface charge has the effect of canceling out some of the piezoelectric field. An alternative assumption therefore would be to assume that enough charge is transferred between the interfaces to balance out the piezoelectric field and symmetrize the structure. In this case the calculated band overlap is very similar (only 3 meV different), since the dominant factors in the calculation are the high electron and hole densities found for the [111]-oriented structures.

As soon as any pressure is applied all the holes are lost from one of the interfaces, the depletion field on this side of the InAs well is reduced, and the GaSb valence band no longer bends up to reach the Fermi energy. It is possible to determine the interface charge, but the values are spread quite widely and show no clear variation with pressure. When all the holes have disappeared, the depletion field is unknown for the GaSb regions on either side of the InAs well and it is no longer possible to calculate the interface charge. The overlap that we deduce in this regime is very dependent on the interface charge, but unfortunately we cannot predict this charge using the lower pressure points. However, for the pressure values with zero hole density it is still possible to give a maximum value for the band overlap, since the GaSb valence band does not bend up above the Fermi energy on either side of the InAs well, or the hole density would not be zero. The band overlap has been calculated for all the points with nonzero hole densities and the results are plotted in Fig. 6, together with the upper limits for the higher pressures, when $n_h = 0$. The overall conclusion from this is that the pressure coefficient of the [111]A overlap is (-11.9 ± 1.5) meV/kbar, which is higher than (-9.9 ± 1.0) meV/kbar found for [001], but the larger zero pressure band overlap still means that the zero overlap condition where the band edges cross is at a higher pressure for [111]A (17±2) kbar than for [001] (14±1.5) kbar.

For [111] growth, atomic planes perpendicular to this direction are composed solely of either anions or cations. These planes are alternately connected by bonds parallel to the [111] direction and three times as many bonds inclined at 70.5° to that direction. This results in an asymmetry in the local environment at a [111] interface, leading to the possible formation of an interface dipole, which will influence the band overlaps. The switching sequence used during the growth of these structures is thought to lead to the formation of a monolayer of InSb at the interface, which has been observed using Raman measurements.[11] For the case of a single monolayer of InSb at the interface, we calculate that a transfer of 1% of an electron charge between each pair of InSb atoms is needed to produce a dipole contribution to the band overlap of 50 meV.[22] It is likely that interface dipole effects are significantly smaller in [001]-oriented structures, where Foulon and Priester[23] have predicted that for a GaSb/InAs interface the band overlap is about 20 meV larger if the interface bond is Ga-As than if it is In-Sb. The orientation dependence of the offsets is likely to be particularly large in the InAs/GaSb system because both the anion and the cation change at the interface. Furthermore, the bulk modulus of InSb is 20% smaller than that of either GaSb or InAs, and will therefore be compressed more by the applied hydrostatic pressure. This is possibly the reason why the [111]A overlap decreases at a faster rate with pressure than the [001] overlap.

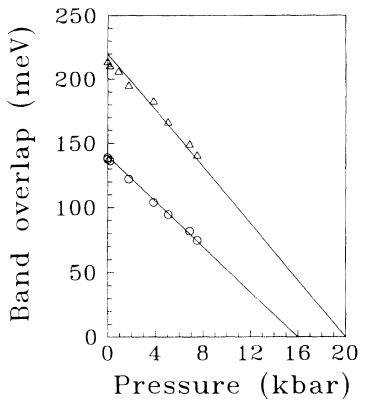

FIG. 7. The band overlaps as functions of pressure for the [001] SL (○) and the [111]*A* shorter period SL (△).

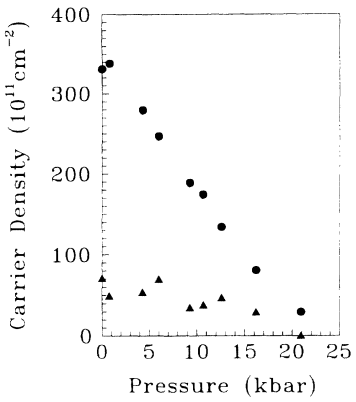

FIG. 8. The densities of electrons (●) and holes (▲) as functions of pressure for the 20 period [111]*A*-oriented SL with layer thicknesses of 960 Å and 480 Å for the GaSb and InAs, respectively.

IV. SUPERLATTICE SAMPLES

Three superlattice samples have also been measured under applied hydrostatic pressure. The samples all had 20 periods and the thicknesses of the layers are given in Table I. The two shorter period SL's were mounted simultaneously in a wider bore cell. Their electron densities were found to decrease at constant rates with pressure, but at slower relative rates than found for the DHET stuctures. The band overlap versus pressure for these samples has been calculated using the fitted electron and hole densities and is shown in Fig. 7. The holes are now confined in a square well with a bowed bottom, as well as the electrons. For the [111]*A* SL both the InAs and GaSb layers are now strained and the piezoelectric fields are 1.9×10^4 V cm^{-1} in the InAs layers and -4.7×10^4 V cm^{-1} in the GaSb calculated following the method of Smith.[7]

These SL samples show the same trend as the DHET samples described earlier, with the band crossing considerably larger for the [111]*A* orientation and decreasing at a slightly larger rate for [111]*A* when compared to the [001] orientation. The pressure coefficients of the band overlaps are similar to those calculated for the DHET data. The zero overlap condition is found by extrapolation to be (16±2) and (20±3) kbar for [001] and [111]*A*, in reasonable agreement with the values of (14±1.5) and (17±2) kbar deduced from the DHET measurements. The errors are increased for the SL samples due to the large extrapolation to higher pressures and also these SL values are not as reliable as those deduced from the DHET data because of uncertainties which may be introduced due to possible variations in the layer thicknesses.

Figure 8 shows the fitted electron and hole densities of the third SL sample measured up to an applied pressure of over 20 kbar. The electron density is again seen to decrease at a constant rate, while holes are present, and a linear extrapolation to zero electron density gives a pressure of (20±2) kbar, above which the hole density will also have fallen to zero. It is difficult to calculate the band overlap for this sample because we can no longer assume that there is no depletion field in the GaSb layers and we do not know accurately the density of dopants. Nevertheless the pressure corresponding to zero electron density is more precisely defined experimentally than for the other [111]*A* SL and should correspond to the zero overlap condition. The pressure value for this is consistent with both of the other [111]*A* structures studied.

V. CONCLUSION

We have used magnetotransport measurements performed under applied hydrostatic pressure to estimate the band crossing for both the [001] and [111]*A* orientations in several different InAs/GaSb heterostructures. The results demonstrate that the band overlap is substantially larger for the [111]*A* orientation in this system. The overlap is found to decrease at a rate of (9.9±1.0) meV/kbar for the [001] orientation but at (11.9±1.5) meV/kbar for the [111]*A* orientation, which is much more rapid than found in earlier measurements, but in agreement with theoretical predictions. Uncrossing of the overlapping conduction and valence bands is found to occur at 14 and 17 kbar for DHET structures grown on the [001] and [111]*A* orientations, respectively, while for superlattices the uncrossing occurs in the region of 16 kbar for [001] and 20 kbar for [111]*A*.

ACKNOWLEDGMENTS

We wish to thank T.-Y. Seong and G. R. Booker for the TEM measurements and K. R. Belcher and S. Moulder for technical assistance. This work was supported by the Science and Engineering Research Council (UK).

[1]L. L. Chang, J. Phys. Soc. Jpn. **49**, 997 (1980).
[2]M. Altarelli, J. C. Maan, L. L. Chang, and L. Esaki, Phys. Rev. B **35**, 9867 (1987).
[3]J. Luo, H. Munekata, F. F. Fang, and P. J. Stiles, Phys. Rev. B **38**, 10 142 (1988).
[4]J. Beerens, G. Grégoris, S. Ben Amor, J. C. Portal, E. E. Mendez, L. L. Chang, and L. Esaki, Phys. Rev. B **35**, 3039 (1987).
[5]N. J. Kawai, L. L. Chang, G. A. Sai-Halasz, C. A. Chang, and L. Esaki, Appl. Phys. Lett. **36**, 369 (1980).
[6]R. J. Nicholas, K. S. H. Dalton, M. Lakrimi, C. López, R. W. Martin, N. J. Mason, G. M. Summers, G. M. Sundaram, D. M. Symons, P. J. Walker, R. J. Warburton, M. I. Eremets, D. J. Barnes, N. Miura, L. Van Bockstal, R. Bogaerts, and F. Herlach, Physica B **184**, 268 (1993).
[7]D. L. Smith, Solid State Commun. **57**, 919 (1986).
[8]M. Lakrimi, R. W. Martin, C. López, D. M. Symons, E. T. R. Chidley, R. J. Nicholas, N. J. Mason, and P. J. Walker, Semicond. Sci. Technol. **8**, S367 (1993), and references therein.
[9]M. Lakrimi, R. W. Martin, N. J. Mason, R. J. Nicholas, and P. J. Walker, J. Cryst. Growth **110**, 677 (1991).
[10]M. Lakrimi, N. J. Mason, R. J. Nicholas, and P. J. Walker, J. Cryst. Growth **124**, 395 (1992).
[11]C. López, R. J. Springett, R. J. Nicholas, P. J. Walker, N. J. Mason, and W. Hayes, Surf. Sci. **267**, 176 (1992).
[12]The classical expression for the Hall voltage was used, as in R. A. Smith, *Semiconductors* (Cambridge University Press, Cambridge, England, 1978), pp. 114 and 115.
[13]E. E. Mendez, L. Esaki, and L. L. Chang, Phys. Rev. Lett. **55**, 2216 (1985).
[14]R. W. Martin, M. Lakrimi, S. K. Haywood, R. J. Nicholas, N. J. Mason, and P. J. Walker, in *High Magnetic Fields in Semiconductor Physics III*, edited by G. Landwehr (Springer-Verlag, Berlin, 1992), p. 420.
[15]T. Ando, A. B. Fowler, and F. Stern, Rev. Mod. Phys. **54**, 437 (1982).
[16]G. M. Sundaram, R. J. Warburton, R. J. Nicholas, G. M. Summers, N. J. Mason, and P. J. Walker, Semicond. Sci. Technol. **7**, 985 (1992).
[17]E. T. R. Chidley, S. K. Haywood, A. B. Henriques, N. J. Mason, R. J. Nicholas, and P. J. Walker, Semicond. Sci. Technol. **6**, 45 (1991).
[18]J. Beerens, G. Grégoris, J. C. Portal, E. E. Mendez, L. L. Chang, and L. Esaki, Phys. Rev. B **36**, 4742 (1987).
[19]L. M. Claessen, J. C. Maan, M. Altarelli, P. Wyder, L. L. Chang, and L. Esaki, Phys. Rev. Lett. **57**, 2556 (1986).
[20]C. G. Van de Walle, Phys. Rev. B **39**, 1871 (1989).
[21]M. Lakrimi, C. López, R. W. Martin, G. M. Summers, G. M. Sundaram, K. S. H. Dalton, N. J. Mason, R. J. Nicholas, and P. J. Walker, Surf. Sci. **263**, 575 (1992).
[22]D. M. Symons, M. Lakrimi, R. J. Warburton, R. J. Nicholas, N. J. Mason, P. J. Walker, and M. I. Eremets, Semicond. Sci. Technol. **9**, 118 (1994).
[23]Y. Foulon and C. Priester, Phys. Rev. B **45**, 6259 (1992).